JCTC Journal of Chemical Theory and Computation

Many-Body Perturbation Theory Extended to the Quantum Mechanics/Molecular Mechanics Approach: Application to Indole in Water Solution

Adriano Mosca Conte,[†] Emiliano Ippoliti,[‡] Rodolfo Del Sole,[†] Paolo Carloni,*[,‡,§] and Olivia Pulci[†]

NAST, ETSF, CNR INFM-SMC, Department of Physics, Universita' di Roma Tor Vergata, Via della Ricerca Scientifica 1, Roma, Italy, Democritos, SISSA—Scuola Internazionale Superiore di Studi Avanzati, via Beirut 2-4, I-34014 Trieste, Italy, and Italian Institute of Technology, SISSA Unit, Via Beirut 2—4, Trieste, Italy

Received December 3, 2008

Abstract: Optical properties of aromatic chromophores are used to probe complex biological processes, yet how the environment tunes their optical properties is far from being fully understood. Here we present a method to calculate such properties on large-scale systems, like biologically relevant molecules in aqueous solution. Our approach is based on many-body perturbation theory combined with a quantum mechanics/molecular mechanics (QM/MM) approach. We include quasiparticle and excitonic effects for the calculation of optical absorption spectra in a QM/MM scheme. We apply this scheme, together with the well-established TDDFT approach, to indole in water solution. Our calculations show that the solvent induces a red shift in the main spectral peak of indole, in quantitative agreement with the experiments, and they point to the relevance of both the electrostatic and geometrical origin of the shift.

1. Introduction

Optical properties of aromatic chromophores embody a key facet of cell biology, allowing for a precise interrogation of a variety of biochemical events, including signaling, metabolism, and aberrant processes. These range from probing transient interactions between biomolecules (proteins and nucleic acids), to protein dynamics and fibrillation and plaque formation in neurodegenerative diseases. Understanding how the environment tunes such optical properties is therefore crucial, yet this information is so far mostly lacking. A powerful tool to address this issue is given by the so-called quantum mechanics/molecular mechanics (QM/MM) methods.[1,2] In this approach, the aromatic moiety may be treated at the quantum mechanical level, while the environment is described with an effective potential: the influence of the MM (presumably very complex and very large) environment is basically included as an external potential and, in case the chromophore is covalently bound to MM region, by a mechanical coupling with the environment.

Most often the QM approach is solved within density functional theory (DFT)[3,4] to study ground state properties, and time-dependent DFT (TDDFT)[5,6] when excited states are involved, as in the case of the optical properties.[7–9] TDDFT is computationally very efficient, yet its predictive power depends dramatically on the system and on the functional used to reproduce the exchange and correlation interactions.

Several approaches, including post-Hartree—Fock ones[10] (configuration interaction and similar methods), have been already used to predict optical properties of biomolecules. Many-body perturbation theory (MBPT),[11,12] is an attractive alternative, although of course it comes with higher computational cost than TDDFT. In fact, TDDFT[13] scales with N^3 ("N" is the number of atoms), while MBPT scales with N^6 (or N^4 in the case where the Haydock algorithm[14] is used). However, biophysical applications of one of the most widely used schemes of MBPT, the combination of the GW

* To whom correspondence should be addressed. E-mail: carloni@sissa.it.

[†] Universita' di Roma Tor Vergata.

[‡] Democritos.

[§] Italian Institute of Technology.

10.1021/ct800528e CCC: $40.75
Published on Web 05/29/2009

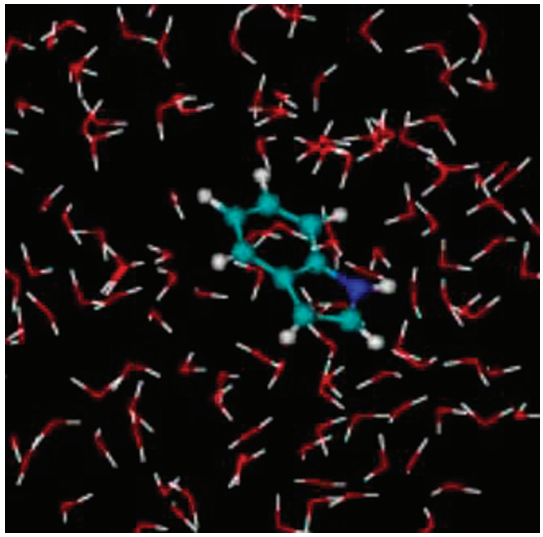

Figure 1. Indole in water solution. Colors correspond to the following atomic species: blue, N; cyan, C; white, H; red, O.

method[11] with the Bethe−Salpeter equation (BSE),[12] are, so far, lacking. The GW method is used for the evaluation of the single quasiparticle energies, and the BSE to introduce excitonic effects. The determination of a more accurate long-range exchange-correlation kernel of TDDFT is also based on MBPT.[15] Keeping in mind this for future biological applications, it is imperative to assess the accuracy of the MBPT/MM approach versus the more conventional TDDFT/MM one.[7,8]

The main assumption in interfacing a QM/MM method with TDDFT or MBPT approaches is that the optical properties of the chromophore do not involve the electronic structure of the MM part. Hence, special care has to be devoted to the choice of the two regions.

Here we present MBPT/MM calculations on the indole ring of the tryptophan residue (Figure 1). This system appears ideal for such an approach in several respects. First, it is very relevant biologically, as the indole ring has been exploited as a spectroscopic tool to monitor changes in proteins[16] and to yield information about local structure and dynamics. In fact, its spectral signatures allow it to be used as a structural probe in proteins. Second, it contains a relatively small number of atoms ($N = 16$), which can be treated quite easily at the GW-BSE level. Next, the optical gap of liquid water (7 eV)[17] is larger than the gap of the indole molecule (4.3 eV).[18] Under 7 eV, the spectra of indole and water do not overlap, and it is justified to treat the solvent in a classical scheme. Finally, CASPT2 calculations[18] and experimental data[19] are available and allow us to compare the changes of the optical properties upon passing from the gas phase to aqueous solution.

2. Methods and Computational Details

We performed QM/MM Car−Parrinello[20] simulations of indole in water by the fully Hamiltonian QM/MM scheme.[2] Such a scheme has been applied to a variety of biological systems.[21] The biomolecule was treated, at this step, at the DFT level, while the solvent was described by the TIP3P water model[22] and the van der Waals parameters on each indole atomic site in the interaction potential were employed by using the Amber force field.[23] This approach allows for an explicit treatment of solvation, in contrast to previous studies.[18,19,24]

Indole single quasiparticle energies have been then evaluated at the GW level for several snapshots. Finally, we solved the BSE to calculate the average absorption spectrum and compared the results with the ones obtained within TDDFT. We calculated the indole absorbance in water as well as in gas phase. The shift in the spectra gives the solvatochromism.

In this section we review the main aspects of the GW methods and of the Bethe−Salpeter equation and explain how it is possible to include these methods in a QM/MM scheme. In 1965, Hedin[25] formulated a set of five equations that link together five important functions: the Green's function, G; the self-energy, Σ; the vertex function, Γ; the polarizability, P; and the screened potential, W. The poles of the Green's function in frequency space are the energies of the states of an ionized system referred to the ground-state energy. Here the ionized system is a system to which an electron has been subtracted or added. These excitation energies are called quasiparticle energies ε_j^{QP} and can be derived by solving the following eigen-problem:

$$\left[-\frac{\hbar^2\nabla^2}{2m} + U^{QM}(\mathbf{r}) + U^{QM/MM}(\mathbf{r}) + V_H(\mathbf{r})\right]\phi_j^{QP}(\mathbf{r}) + \int d^3\mathbf{r}'\,\Sigma(\mathbf{r},\mathbf{r}',\varepsilon_j^{QP})\,\phi_j^{QP}(\mathbf{r}') = \varepsilon_j^{QP}\phi_j^{QP}(\mathbf{r}) \quad (1)$$

This expression is derived from the Dyson equation in the Lehmann representation.[11] V_H is the Hartree potential and U^{QM} is the Coulomb potential generated by the QM ions, while $U^{QM/MM}$ is the potential felt by the electrons due to the point charges of the MM part.

According to Hedin equations, the self-energy is a functional of G, W, and Γ. Several calculations have demonstrated that Γ can be approximated to a delta function for most of the systems.[26] Under this condition, the time-Fourier transform of the proper exchange-correlation self-energy, $\Sigma(\mathbf{r},\mathbf{r}',\omega)$, is a convolution of the Green's function, $G(\mathbf{r},\mathbf{r}',\omega)$, with the screened Coulomb potential, $W(\mathbf{r},\mathbf{r}',\omega)$: $\Sigma = iGW$. This is the reason for the name "GW approximation". In this work, Σ is calculated as the convolution of the noninteracting electron system's Green function (G_0) and the screened Coulomb potential (W_0) built from the Kohn−Sham (KS) eigenvalues and eigenvectors of the QM/MM system, $\varepsilon_j^{QM/MM}$ and $\phi_j^{QM/MM}$, respectively. More explicitly, G_0 in frequency space is

$$G_0(\mathbf{r},\mathbf{r}',\omega) = \sum_j \phi_j^{QM/MM}(\mathbf{r})\,\phi_j^{QM/MM*}(\mathbf{r}') \left[\frac{\theta(\varepsilon_j^{QM/MM} - \varepsilon_F)}{\omega - \varepsilon_j^{QM/MM} + i\eta} + \frac{\theta(\varepsilon_F - \varepsilon_j^{QM/MM})}{\omega - \varepsilon_j^{QM/MM} - i\eta}\right] \quad (2)$$

where ε_F is the Fermi energy. The screened potential is evaluated as $W = \varepsilon^{-1}v$, where v is the bare Coulomb potential and ε is the microscopic dielectric function at the independent particle level.

Equation 1 has the same form as the KS equation[4] in the presence of an external field, where the exchange-correlation potential $V_{xc}^{DFT}(\mathbf{r})$ is replaced by the self-energy $\Sigma(\mathbf{r},\mathbf{r}',\varepsilon_j^{QP})$, which acts as a nonlocal, energy-dependent potential. Therefore, the eigenvalue problem described above can be solved perturbatively considering the KS Hamiltonian as an unperturbed Hamiltonian and $\Sigma - V_{xc}$ as a perturbative term. The quasiparticle eigenvalues are obtained in first-order perturbation theory:

$$\varepsilon_j^{QP} = \varepsilon_j^{QM/MM} + \frac{\langle \phi_j^{QM/MM} | \Sigma(\varepsilon_j^{QM/MM}) - V_{xc} | \phi_j^{QM/MM} \rangle}{1 - \langle \phi_j^{QM/MM} | \frac{d\Sigma(\omega)}{d\omega}\Big|_{\omega=\varepsilon_j^{QM/MM}} | \phi_j^{QM/MM} \rangle} \quad (3)$$

All the Coulomb interactions, and hence also the one induced by the classical MM region, are included in the KS eigenvalues $\varepsilon_j^{QM/MM}$ and eigenvectors $|\phi_j^{QM/MM}\rangle$.

The quasiparticle energies obtained by the GW method and the QM/MM eigenfunctions $\phi_j^{QM/MM}(\mathbf{r})$ are then used to calculate the optical absorption spectrum through the solution of the BSE equation:

$$P(1,1',2,2') = P_{IQP}(1,1',2,2') + \int P_{IQP}(1,1',3,3')\,\Xi(3,3',4,4')\,P(4,4',2,2')\,d(3,3',4,4') \quad (4)$$

where $1 \equiv \mathbf{r}_1, t_1$ (and similarly for 1′, 2, 2′, etc.) and P_{IQP} is a generalized four-point irreducible polarizability and describes the propagation of independent quasielectron and quasihole couples (for a review, see ref 12). All the interactions are contained in the kernel Ξ, defined as

$$\Xi(1,1',2,2') = \delta(1,1')\,\delta(2,2')\,v(1,1') - \delta(1,1')\,\delta(1',2')\,W(1,1') \quad (5)$$

The kernel Ξ is made of two parts, v and W, resulting from the functional derivative of the Hartree potential and of the self-energy with respect to the single-particle Green's function, respectively. v is the electron−hole exchange, and W is the term responsible for bound excitons.

In practice, to solve the BSE, the problem is recast into an effective two-body Hamiltonian form:

$$H_{exc}^{(n_1,n_2),(n_3,n_4)} = (\varepsilon_{n_2}^{QP} - \varepsilon_{n_1}^{QP})\delta_{n_1,n_3}\delta_{n_2,n_4} + (f_{n_1} - f_{n_2}) \int d\mathbf{r}_1 \int d\mathbf{r}'_1 \int d\mathbf{r}_2 \int d\mathbf{r}'_2\, \phi_{n_1}^{QM/MM*}(\mathbf{r}_1)\,\phi_{n_2}^{QM/MM}(\mathbf{r}'_1) \times \Xi(\mathbf{r}_1,\mathbf{r}'_1,\mathbf{r}_2,\mathbf{r}'_2)\,\phi_{n_3}^{QM/MM}(\mathbf{r}_2)\,\phi_{n_4}^{QM/MM*}(\mathbf{r}'_2) \quad (6)$$

where f_n is the occupation number of level n. Hence, using the spectral representation[27] for the inverse of a matrix, the interacting polarization can be obtained by solving an effective eigenvalue problem:

$$\sum_{n_3,n_4} H_{exc}^{(n_1,n_2),(n_3,n_4)} A_\lambda^{(n_3,n_4)} = E_\lambda A_\lambda^{(n_1,n_2)} \quad (7)$$

The optical spectrum assumes then the following form:

$$\varepsilon_M(\omega) = 1 - \lim_{q\to 0} v(\mathbf{q}) \sum_{\lambda,\lambda'} \left[\sum_{n_1,n_2} \langle n_1 | e^{-i\mathbf{qr}} | n_2 \rangle \times \frac{A_\lambda^{(n_1,n_2)}}{\omega - E_\lambda + i\eta} N_{\lambda,\lambda'}^{-1} \times \sum_{n_3,n_4} \langle n_4 | e^{-i\mathbf{qr}} | n_3 \rangle A_{\lambda'}^{*(n_1,n_2)} (f_{n_3} - f_{n_4}) \right] \quad (8)$$

where

$$N_{\lambda,\lambda'}^{-1} = \sum_{n_1,n_2} A_\lambda^{*(n_1,n_2)} A_{\lambda'}^{(n_1,n_2)} \quad (9)$$

The BSE can be physically interpreted as adding the electron−hole interaction to the energy of the excited state of the system. An electron−hole pair is called an exciton and its contribution to the optical spectrum (obtained by solving the BSE) gives the so-called excitonic effects. Since the electron−hole interaction is attractive, it affects the DFT+GW optical spectrum mainly with a red shift of the peaks. Moreover, electron−hole bound states (the excitons) occur below the single-particle gap. The difference between the DFT+GW electronic gap and the excitonic optical gap measures the exciton binding energy. The quantum plus classical external potential is not explicitly present in the BSE but indirectly determines all its ingredients via the quasiparticle energies and wave functions.

To take into account solvation and temperature (300 K) effects, we performed a 20 ps hybrid QM/MM Car−Parrinello simulation of a system where the QM part was the indole molecule and the MM part was 1376 water molecules.[28]

For 10 snapshots of the QM/MM dynamics (one every 2 ps) we computed the optical spectra at the independent particle level (DFT-IPA) and within TDDFT.[29] The running average of the spectra indicates that, at the DFT level and for a dynamics of 20 ps, the convergency of the spectrum with the number of snapshots is achieved after six snapshots. We confirmed this statement by a comparison with a spectrum averaged over 120 snapshots. A better sampling could be obtained by performing several dynamics and repeating the test by using TDDFT and/or GW-BSE, but this goes beyond our computational possibilities. Hence, the subsequent GW and BSE calculations have been performed on only six snapshots (atomic coordinates are in the Supporting Information).

3. Results and Discussion

HOMO−LUMO Gaps. Our calculated DFT and GW HOMO−LUMO gaps[30] averaged over the QM/MM configurations, resulted to be 3.8 eV (with standard deviation $\sigma = \pm 0.1$ eV) and 7.2 eV ($\sigma = \pm 0.2$), respectively. The HOMO−LUMO gap calculated by the GW method corresponds to the electronic gap and not to the optical gap. The GW correction to the electronic gap, during the dynamics, ranges from 3.3 to 3.5 eV. Therefore, its value can in principle be calculated for just one snapshot, and used, with an error of 0.2 eV, for all the other frames. This fact, already found for liquid water,[17] confirms that one can strongly reduce the computational effort, by performing a GW calculation for just one snapshot. However, this error would be too large for our purpose of evaluating the solvent shift.

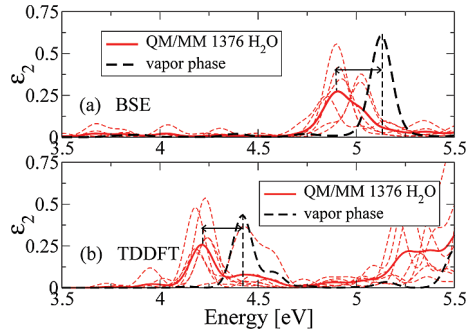

Figure 2. BSE (a) and TDDFT (b) spectra of indole in water. The tiny red dashed lines are the spectrum of each snapshot. The red solid line is obtained by an average over these spectra. The black dashed line is for indole in vapor phase.

As a consequence, in this work the GW corrections of the electronic gap have been calculated for each single snapshot.

Optical Spectrum. We next calculated the low-energy range of the optical spectrum of indole, by GW-BSE[31] and TDDFT, always as a result of an average over the QM/MM snapshots. In Figure 2 we report our results together with the calculated absorption spectrum in the gas phase. In our TDDFT calculations, the most intense peak (which corresponds to the ^1L_a transition located at 4.77 eV in the experimental spectrum)[19] is mainly due to an HOMO−LUMO transition, in agreement with previous calculations performed by CASSCF-CASPT2 methods.[18,32] The analysis of the charge distribution of the electronic levels reveals the $\pi-\pi^*$ character of this transition and an electronic charge depletion around the nitrogen atom on passing from the HOMO to the LUMO.

We notice that, in both TDDFT and GW-BSE approaches, this peak is red-shifted on passing from gas phase to the water solution. The value we calculate for such a red shift is ∼0.2 eV in both cases, in good agreement with the experiment (0.18 eV).[19] A similar trend was obtained by previous theoretical calculations of indole in water based on CASSCF-CASPT2 methods.[18] In these approaches, the indole configuration was the one obtained after a geometry optimization, with the solvent simulated by a continuum model, with a cavity containing the molecule. The CASSCF-CASPT2 prediction for the solvent shift is about 0.06 eV only. Such an underestimation may depend on the different geometrical conformation of indole molecule in the gas phase and in water, caused by the interaction with the solvent (which was not considered explicitly in).[18] In fact, in our calculations, comparison of the indole geometries in all the snapshots with that of the stable conformation in the gas phase (defined as the equilibrium geometry in vacuum) shows a slight loss of planarity (the dihedral angle between the planes of the two rings of indole is below 6°). Moreover, compared to the gas-phase configuration, the C−C bond lengths of indole in water can differ up to 4% and their average value is 1%−2% larger than the one calculated for the relaxed configuration. The angles differ by 1°−4° with respect to the gas-phase configuration. These geometrical changes are small but can significantly affect the optical properties, since they involve the breaking of some symmetries.

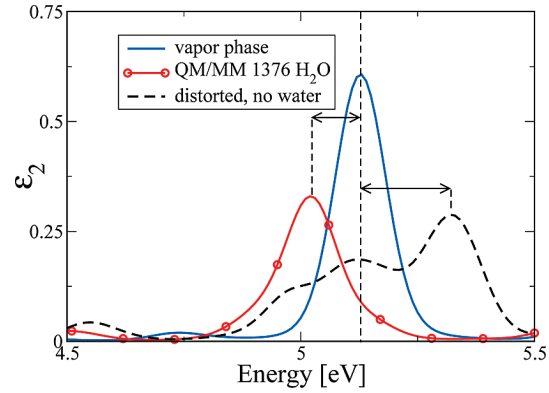

Figure 3. BSE optical spectra: solid blue line, indole in vapor phase; black dashed line, indole without water molecules, with atomic coordinates taken from a snapshot corresponding to 13.08 ps of the dynamics; circles, indole in water, with the spectrum calculated for the same snapshot.

To quantify the contribution of these effects on the solvent shift, we performed GW-BSE calculations of the optical absorption spectrum of indole switching on and off the water field, in order to separate the geometry effect from the electrostatic one. The results are presented for a single snapshot in Figure 3. The corresponding solvent shift goes from −0.1 eV with water field to +0.2 eV (hence, a blue shift) without water field. This emphasizes the importance of taking into account explicitly the electrostatic interaction with the solvent, since the geometry distortion alone would give, at least for this snapshot, a wrong sign.

In our calculations, TDDFT underestimates the energy of the ^1L_a peak[19] with respect to experiments, both in gas phase and in solution by ∼0.4 eV, and GW-BSE overestimates them by ∼0.3 eV. Concerning the gas phase, a result closer to the experiment is obtained by using a B3LYP functional[33] with a localized basis set; the underestimation in this case drops to 0.05 eV. We note that for this system the predictive power of TDDFT is comparable to MBPT. This was expected, since TDDFT is usually very efficient for small molecules such as indole (except in some particular cases).[34] Therefore, beside being a relevant biological molecule, indole is also a good system for the main purpose of this work, that is, the introduction and validation of a new scheme (GW-BSE/MM) by comparing the results with the experiments and with well-working methods on a relevant biological system.

As expected,[24] CASSCF is worse in predicting the energy position of the first peak of the absorption spectrum. It overestimates it by almost 1 eV or more, while CASPT2 is more accurate (∼0.13 eV for the gas phase). All the experimental and theoretical values obtained by different methods concerning the indole ^1L_a transition are summarized and compared in Table 1.

Role of the Solute−Solvent H-Bond. The indole N−H moiety is the only group that can form a hydrogen bond with the solvent molecules. In this section, we investigate qualitatively the role of the H-bond for the solvatochromism by performing TDFFT calculations of the optical absorption spectrum. These calculations are of course much cheaper than the GW calculations.

Table 1. Theoretical and Experimental Transition Energy (in eV) of the ^1L_a Peak of Indole Spectrum in Gas Phase and in Water and Their Difference

	MBPT/MM[a]	TDDFT/MM[a]	CASPT2[b]	EXP[c]
gas phase	5.1	4.4	4.73	4.77
in water	4.9	4.2	4.67	4.59
solvent shift	0.2	0.2	0.06	0.18

[a] This work. [b] Reference 19. [c] Reference 18.

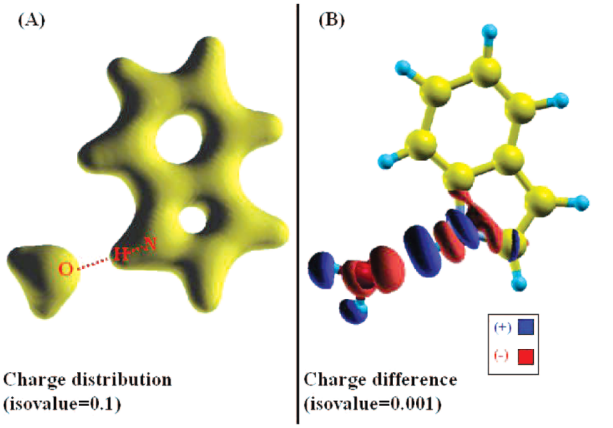

Figure 4. Indole and the water molecule involved in the H-bond. (A) The electronic charge distribution. (B) The difference in the charge distribution between the entire system and the two separated subsystems: isolated indole and isolated water molecule. This enables us to visualize the increasing of the polarization induced by the H-bond.

The geometry of the H-bond can be evinced by the calculation of distribution functions calculated from the QM/MM trajectory. The first maximum and minimum of the radial distribution function (rdf) between N and water oxygens O_w are 2.96 and 3.20 Å, respectively. The maximum of N−H···O_w angle, as obtained from the correspondent angular distribution function, is 155° (radial and angular distribution functions are available in the Supporting Information). This result agrees with force-field-based molecular dynamics simulation of indole in a large water box (∼10 000 solvent molecules) performed here[35] as well as with previous results reported in the literature.[36]

We then selected a representative QM/MM snapshot (Figure 4), in which the N−H···O_w distance is 2.91 Å, very close to that of the first rdf peak. In addition, in this snapshot the N−H···O_w angle is 155°; this value is similar to the maximum of the correspondent angular distribution function.

We performed on this snapshot TDDFT calculations of the optical spectrum. The calculations differed for the MM external potential $U^{QM/MM}$: $U^{QM/MM}$ is either generated by a water molecule (WAT hereafter) involved in the H-bond (i), or by all water molecules (ii), or it is zero (iii). By comparing the spectrum of i with that of iii, we conclude that the H-bond induces a small red shift (<0.1 eV) on the ^1L_a peak in this representative snapshot (Figure 5). By comparing the spectrum of ii with that of iii we observe a shift larger than 0.3 eV. On the basis of these calculations, we suggest therefore that the H-bond plays a role in the solvatochromism and that a considerable effect is given by the bulk solvent. The latter has to be included to obtain a quantitative evaluation of the solvent shift.

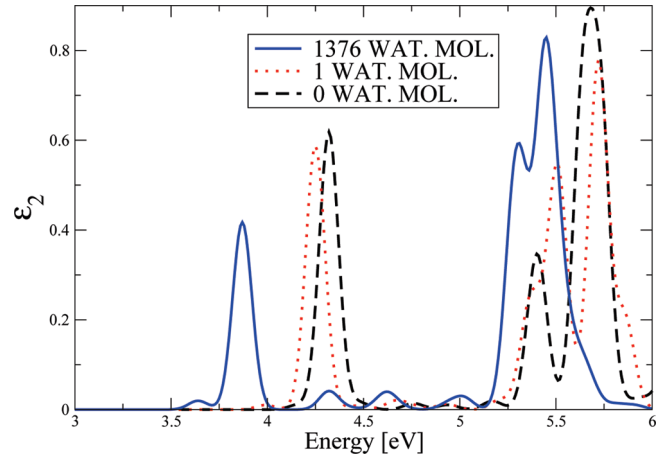

Figure 5. TDDFT absorption spectrum of indole in water. Spectra are calculated for a selected snapshot (see the text). Water molecules are treated classically.

Of course, solvent polarization and charge transfer effects associated with the H-bond might affect the solvatochromism. We addressed this issue by switching on the QM character of WAT in calculation ii. In other words, we performed a calculation in which WAT molecule was treated at the TDDFT level as indole, and all the other were treated classically. A Löwdin charge analysis[37] points to the absence of charge transfer effects between indole and WAT, while polarization effects are present (see Figure 4). The change in absorption peak ^1L_a relative to calculation ii is very small (less than 0.02 eV). The same results were obtained by including also a second water molecule. Thus, polarization effects, although sizable, do not affect largely the absorption spectrum. Our conclusions agree with TDDFT/MM calculations performed for another organic molecule in water solution: acetone.[38] Like indole, this molecule forms H-bonds with the solvent. The calculated absorption spectrum is almost the same when the solvation sphere of 12 water molecules surrounding acetone are treated by a QM or MM approach. The approximation of treating the solvent at a classical level allows us to avoid small box size effects and sample much longer time scales than using a fully ab initio scheme. This is absolutely crucial already for this small system. It is expected to be even more relevant for large biological systems.

4. Summary

In this paper, we have included many-body perturbation theory in a QM/MM scheme. We have applied it, together with a TDDFT/MM approach, to study the optical properties of indole in water solution. Both methods reproduce quantitatively the red shift induced by the solvent. The GW-BSE/MM method can be applied to biomolecules in aqueous solution (i.e., in laboratory-realizable conditions), although with a larger computational cost (for this particular case, MBPT requires 8 times more CPU time than TDDFT to calculate the indole optical spectrum).

Many works put in evidence the GW-BSE method to be a possible alternative to TDDFT to treat large size materials

or charge transfer systems.[39] We expect the GW-BSE, whose range of applications has been here extended to molecules in solution and in different chemical environments, to be able to study long-range charge-transfer molecules in their biochemical environment.[40,41] Moreover, a better exchange and correlation kernel can be derived from MBPT to improve TDLDA/GGA.[15]

Our calculations show that the solvent shift is a consequence of the combination of two effects: the geometrical distortion of indole molecule in the solvent and the electrostatic interaction with the water molecules' electric dipoles. Both effects, and their sum, depend on the particular configuration of the system; this emphasizes the need of including *both* altogether and of averaging over several snapshots.

This work opens the way to further applications of MBPT/MM to other biorelevant molecules, such as fluorescent probes in their target proteins, for which the evaluation of the optical shift enables the understanding of the nature of their environment.

Acknowledgment. We acknowledge support from EU e-13 ETSF Project 211956. Computer resources from INFM "Progetto Calcolo Parallelo" at CINECA are gratefully acknowledged. We also thank L. Guidoni for interesting discussions.

Supporting Information Available: PDB file including most of the snapshots of the QM/MM trajectory used for the calculations; radial distribution function calculated from the QM/MM trajectory between the nitrogen of the indole and water oxygens; angular distribution function for the angle formed by the nitrogen of the indole, its hydrogen, and the oxygens in the corresponding first shell of water. This material is available free of charge via the Internet at http://pubs.acs.org.

References

(1) Carter, E. A.; Hynes, J. T. *J. Chem. Phys.* **1991**, *94*, 5961–1129.

(2) Laio, A.; VandeVondele, J.; Röthlisberger, U. *J. Chem. Phys.* **2002**, *116*, 6941.

(3) Hohenberg, P.; Kohn, W. *Phys. Rev.* **1964**, *136*, B864.

(4) Kohn, W.; Sham, L. J. *Phys. Rev.* **1965**, *140*, A1133.

(5) Runge, E.; Gross, E. K. U. *Phys. Rev. Lett.* **1984**, *52*, 997.

(6) Marques, M. A. L.; Gross, E. K. U. Time-Dependent Density Functional Theory. In *A Primer in Density Functional Theory*; Fiolhais, C., Nogueira, F., Marques, M. A. L., Eds.; Springer-Verlag: Berlin, 2003; Vol. 620, pp 144−184.

(7) Sulpizi, M.; Carloni, P.; Hutter, J.; Röthlisberger, U. *Phys. Chem. Chem. Phys.* **2003**, *5*, 4798.

(8) Sulpizi, M.; Röhrig, U. F.; Hutter, J.; Röthlisberger, U. *Int. J. Quantum Chem.* **2004**, *101*, 671.

(9) Moret, M.-E.; Tapavicza, E.; Guidoni, L.; Röhrig, U. F.; Sulpizi, M.; Tavernelli, I.; Röthlisberger, U. *CHIMIA Int. J. Chem.* **2005**, *59*, 493–498.

(10) Frutos, L. M.; Andruniów, T.; Santoro, F.; Ferré, N.; Olivucci, M. *Proc. Natl. Acad. Sci. U.S.A.* **2007**, *104*, 7764.

(11) Fetter, A.; Walecka, J. *Quantum Theory of Many-Particle Systems*; McGraw-Hill: San Francisco, 1971; pp 1−197.

(12) Onida, G.; Reining, L.; Rubio, A. *Rev. Mod. Phys.* **2002**, *74*, 601.

(13) TDDFT, as implemented in the CPMD code[42] used in this work, uses the Tamm−Dancoff approximation.

(14) Haydock, R. *Comput. Phys. Commun.* **1980**, *20*, 11.

(15) Botti, S.; Shindlmayr, A.; Del Sole, R.; Reining, L. *Rep. Prog. Phys.* **2007**, *70*, 357, and references therein.

(16) Creed, D. *Photochem. Photobiol.* **1984**, *39*, 537.

(17) Garbuio, V.; Cascella, M.; Reining, L.; Del Sole, R.; Pulci, O. *Phys. Rev. Lett.* **2006**, *97*, 137402, and references therein.

(18) Serrano-Andres, L.; Roos, B. O. *J. Am. Chem. Soc.* **1996**, *118*, 185, and references therein.

(19) Lami, H. *J. Chem. Phys.* **1977**, *67*, 3274.

(20) Car, R.; Parrinello, M. *Phys. Rev. Lett.* **1985**, *55*, 2471.

(21) Peraro, M. D.; Ruggerone, P.; Raugei, S.; Gervasio, F. L.; Carloni, P. *Curr. Opin. Struct. Biol.* **2007**, *17*, 149.

(22) Jorgensen, W. L.; Chandrasekhar, J.; Madura, J. D.; Impey, R. W.; Klein, M. L. *J. Chem. Phys.* **1983**, *79*, 926.

(23) Pearlman, D. A.; Case, D. A.; Caldwell, J. W.; Ross, W. S.; Cheatham, T. E.; Debolt, S.; Ferguson, D.; Seibel, G.; Kollman, P. *Comput. Phys. Commun.* **1995**, *91*, 1.

(24) Rogers, D. M.; Hirst, J. D. *J. Phys. Chem.* **2003**, *107*, 11191.

(25) Hedin, L. *Phys. Rev.* **1965**, *139*, A796.

(26) Aryasetiawan, F.; Gunnarsson, O. *Rep. Prog. Phys.* **1998**, *61*, 237–312.

(27) Albrecht, S.; Reining, L.; Del Sole, R.; Onida, G. *Phys. Rev. Lett.* **1998**, *80*, 4510.

(28) The QM/MM code[2] combines the CPMD3.11.1 and the P3M version of the GROMOS code.[43] This is a dual simulation box QM/MM method: QM solute and MM solvent are defined on periodically replicated simulation cells of different sizes. The QM cell size is $11.8 \times 10.8 \times 12.5$ Å^3 and it is immersed in a box of $33.7 \times 35.1 \times 35.6$ Å^3 containing 1376 TIP3P water molecules. Electrostatic interaction between periodic images of the QM part is decoupled by the scheme of Martyna−Tuckerman.[44] The electrostatic interaction of the classical part with periodic boundary conditions is treated by the particle−particle, particle−mesh method: we checked that the size of the box was large enough to prevent the solute from interacting with its images, estimating such interaction energy in the presence of the water and comparing it with the thermal energy fluctuation. We used BLYP pseudopotentials corrected for a better description of van der Waals interactions,[45] 70 Ry energy cutoff (indole's N−H group forms H-bonds with water), and 0.1 fs time step for the dynamics. A Nose−Hoover thermostat is applied throughout all simulations to keep the temperature constant.

(29) All TDDFT calculations are obtained within the Tamm−Dancoff approximation as implemented in the CPMD 3.11.1 package. For the exchange-correlation kernel, we tested different functionals (LDA, BLYP, BP, PBE), the choice being limited by the use of a plane-wave basis set. On the other hand, plane-wave-based calculations have some advantages when performing molecular dynamics (summarized in ref 46), particularly the ability to efficiently calculate the forces on atoms that are most important in our QM/MM scheme. The same corrected Troullier−Martins pseudopotentials and elec-

trostatic treatment of the classical part as for the dynamics have been used.

(30) GW calculations have been done by using 12 077 plane-waves and 500 electronic bands. Following ref 47, we used periodic boundary conditions and a cutoff in real space for the Coulomb potential to prevent that periodic images interact with each other. The screening function is calculated within a plasmon pole approximation. For MBPT calculations, we used codes developed within the ETSF (www.etsf.eu/resources/software/codes).

(31) The BSE was solved by diagonalizing the excitonic Hamiltonian with the inclusion of the coupling part. We used 12 077 plane-waves for the wave functions, 257 for the local fields, and 5100 quasiparticle transitions. We use periodic boundary conditions with a cutoff in real space for the Coulomb potential.[47]

(32) Borin, A. C.; Serrano-Andres, L. *Chem. Phys.* **2000**, *262*, 253.

(33) Rogers, D. M.; Besley, N. A.; O'Shea, P.; Hirst, J. D. *J. Phys. Chem. B* **2005**, *109* (48), 23061.

(34) Sun, M.; Ding, Y.; Cui, G.; Liu, Y. *J. Phys. Chem. A* **2007**, *111*, 2946.

(35) The indole molecule with a geometry taken after a geometry optimization by using CPMD with 70 Ryd energy cutoff was inserted in a box of 9575 water molecules of around 70 Å edges. The AMBER force field and TIP3P force fields were used for indole and water, respectively. A time step of 1.5 fs was used. The SHAKE algorithm was used to fix the lengths of covalent bonds that involve hydrogens. We used a Langevin dynamics with a collision frequency of 5 ps^{-1} and the isotropic position scaling algorithm to regulate pressure as implemented in the Amber package to sample in a NPT ensemble. Electrostatic interactions were evaluated using the particle mesh Ewald method, with a cutoff for the real part of 12 Å. The same value was used for the cutoff of the van der Waals interactions.

(36) Simonson, T.; Wong, C. F.; Brünger, A. T. *J. Phys. Chem. A* **1997**, *101* (10), 1935.

(37) Löwdin, P.-O. *J. Chem. Phys.* **1950**, *18*, 365.

(38) Röhrig, U. F.; Frank, I.; Hutter, J.; Laio, A.; VandeVondele, J.; Röthlisberger, U. *ChemPhysChem* **2003**, *4*, 1177.

(39) Reining, L.; Olevano, V.; Rubio, A.; Onida, G. *Phys. Rev. Lett.* **2002**, *88*, 066404.

(40) Cai, Z.-L.; Sendt, K.; Reimers, J. R. *J. Chem. Phys.* **2002**, *117*, 5543.

(41) Dreuw, A.; Head-Gordon, M. *J. Am. Chem. Soc.* **2004**, *126*, 4007.

(42) Hutter, J.; Alavi, A.; Deutsch, T.; Ballone, P.; Bernasconi, M.; Focher, P.; Goedecker, S.; Tuckerman, M.; Parrinello, M. *CPMD 3.11.1*; Copyright IBM Corp, 1990−2006; Copyright MPI für Festkörperforschung, Stuttgart, 1997−2001, 2006.

(43) Luty, B. A.; Davis, M. E.; Tironi, I. G.; van Gunsteren, W. F. *Mol. Simul.* **1994**, *14*, 11.

(44) Martyna, G. J.; Tuckerman, M. E. *J. Chem. Phys.* **1999**, *110*, 2810.

(45) von Lilienfeld, O. A.; Tavernelli, I.; Röthlisberger, U.; Sebastiani, D. *Phys. Rev. Lett.* **2004**, *93*, 153004.

(46) Marx, D.; Hutter, J. Ab initio molecular dynamics: Theory and Implementation. In *Modern Methods and Algorithms of Quantum Chemistry*; Grotendorst, J., Ed.; John von Neumann Institute for Computing: Juelich, 2000; Vol. 1, pp 301−449.

(47) Onida, G.; Reining, L.; Godby, R. W.; Del Sole, R.; Andreoni, W. *Phys. Rev. Lett.* **1995**, *75*, 818–821.

CT800528E